

# Lower hybrid destabilization of trapped electron modes in tokamak and its consequences for anomalous diffusion

Animesh Kuley,<sup>1,a)</sup> C. S. Liu,<sup>2</sup> and V. K. Tripathi<sup>1</sup>

<sup>1</sup>Department of Physics, Indian Institute of Technology Delhi, New Delhi 110016, India

<sup>2</sup>Department of Physics, University of Maryland, College Park, Maryland 20742, USA

(Received 11 January 2010; accepted 25 May 2010; published online 15 July 2010)

Parametric coupling of lower hybrid pump wave with low frequency collisionless/weakly collisional trapped electron drift wave, with frequency lower than the electron bounce frequency, is studied. The coupling produces two lower hybrid sidebands. The sidebands beat with the pump to exert a low frequency ponderomotive force on electrons that causes a frequency shift in the drift wave, leading to the growth of the latter. The short wavelength modes are destabilized and they enhance the anomalous diffusion coefficient. © 2010 American Institute of Physics.

[doi:10.1063/1.3454692]

## I. INTRODUCTION

Drift waves driven by trapped electrons, both dissipative trapped electron modes (TEMs) and collisionless TEMs (CTEMs), are considered to be an important agent for anomalous transport in tokamak.<sup>1–14</sup> The nonlinearity associated with the TEMs has been extensively investigated theoretically.<sup>15–19</sup> These microinstabilities are normally investigated using computer codes, e.g., gyrokinetic code GTC,<sup>4,5</sup> GYRO,<sup>6,20</sup> GS2,<sup>21</sup> and EM-GLOGYSTO.<sup>14</sup> The TEM driven turbulence and transport have also been studied experimentally in some tokamaks such as Alcator C-Mod,<sup>21</sup> Axially Symmetric Divertor Experiment (ASDEX) upgrade,<sup>22</sup> and DIII-D.<sup>23</sup>

Recent experiments in Alcator C-Mod<sup>24,25</sup> reported strong modification to toroidal rotation profiles in the core region ( $0 < r/a < 0.4$ ) induced by lower hybrid current drive (LHCD). The change in the radial electric field produced by the LHCD makes a nonambipolar radial current, charging the plasma negatively with respect to its pre-LH state. This appears due to resonant trapped electron pinch, i.e., the canonical angular momentum absorbed by the resonant trapped electrons while interacting with the LH waves and experiencing a faster inward drift than the ions in the core. Liu *et al.*<sup>26</sup> developed an elegant theoretical formalism for radial, cross-field diffusion due to the nonconservation of azimuthal angular momentum in an axisymmetric toroidal system, which appears due to the electric field component along the magnetic field lines of force.

The LH waves launched into a tokamak by a phased array of wave guides and propagating toward the center in a well defined resonance cone are known to excite parametric instabilities. The parametric coupling to ion cyclotron mode and quasimode has been found to be prominent in high density tokamak. The LH wave spectrum thus generated has significant influence over LHCD. The four wave parametric coupling of LH pump wave to drift waves has also been recognized to be important. Liu and Tripathi<sup>27</sup> explained the

suppression of drift waves by four wave parametric process. The  $\mathbf{E} \times \mathbf{B}$  electron drift due to a LH pump wave of finite wave number beats with the density perturbation associated with the drift wave to produce sideband nonlinear currents that drive LH waves at lower and upper sideband frequencies. The sideband waves couple with the pump to exert a ponderomotive force that causes frequency shift in the eigenfrequency of the drift wave. When this frequency shift overcomes the frequency shift due to finite Larmor radius effects, the drift wave is stabilized. The LH pump with a wave number greater than drift wave numbers was shown to stabilize the entire spectrum of drift wave when the pump amplitude exceeds a threshold value. Praburam *et al.*<sup>28</sup> developed a nonlocal theory of this process in a cylindrical plasma column. Wong and Bellan<sup>29</sup> studied the LH wave destabilization of collisional drift wave in the Princeton L-3 device. Redi *et al.*<sup>30</sup> analyzed linear drift mode stability in Alcator C-Mod with radio frequency heating, using GS2 gyrokinetic code, and showed that ion temperature gradient (ITG) and electron temperature gradient modes are unstable outside the barrier region and not strongly growing in the core; in the barrier region ITG/TEM is only weakly unstable for experimental profiles which have been modified by ion cyclotron radio frequency heating.

In a large aspect ratio tokamak, a trapped electron population exists in a fraction of velocity space given by  $\delta\lambda \sim \sqrt{\epsilon}$ , where  $\lambda$  is the particle's pitch angle and  $\epsilon = r/R$  is the inverse aspect ratio of a tokamak magnetic surface with minor and major radii,  $r$  and  $R$ , respectively. The trapped particles complete many bounces in its magnetic well before suffering sufficient small angle collisions to detrapp them. They influence the low frequency drift waves very significantly, and having a destabilizing influence on them. Recently we<sup>31</sup> have carried out the gyrokinetic formalism to study LH wave stabilization of ITG driven modes, in which the longer wavelength drift waves are destabilized by the LH wave while the shorter wavelengths are suppressed. In this paper we study the four wave parametric coupling of a LH pump wave to TEMs.

The paper is organized as follows: in Sec. II the basic

<sup>a)</sup>Electronic mail: animesh47@gmail.com.

model and linear response of pump and sidebands are described. Section III presents low frequency perturbation. Section IV contains the nonlinear response at sidebands and growth rate has been calculated in Sec. V. Finally in Sec. VI we discuss the results.

## II. BASIC MODEL AND LINEAR RESPONSE OF PUMP AND SIDEBANDS

We consider a toroidal geometry with circular concentric magnetic surfaces, parametrized by the usual coordinates  $(\mathbf{r}, \theta, \xi)$  representing the minor radius, poloidal angle, and the toroidal angle coordinates, and the magnetic field can be written as  $\mathbf{B} = B[\mathbf{e}_\xi + (\epsilon/q)\mathbf{e}_\theta]$ , where  $B = B_0(1 - \epsilon \cos \theta)$  is the magnitude of the magnetic field,  $q$  is the safety factor, and  $\mathbf{e}_\xi$  and  $\mathbf{e}_\theta$  are the unit vectors along toroidal and poloidal direction, respectively. The equilibrium distribution functions for electrons and ions are Maxwellians, i.e.,

$$f_{0e}^0 = n(m/2\pi T_e)^{3/2} \exp(-mv^2/2T_e), \quad (1)$$

$$f_{0i}^0 = n(m_i/2\pi T_i)^{3/2} \exp(-m_iv^2/2T_i),$$

where  $m$  and  $m_i$  are the mass of electron and ion,  $v$  is the velocity, and  $T_e$  and  $T_i$  denote the electron and ion temperature, respectively.

A high power LH wave is launched into the plasma with potential  $\phi_0$ ,  $\omega_0$  lies in the range  $\Omega_i \ll \omega_0 \ll \Omega_c$ , and  $\Omega_i$  and  $\Omega_c$  are the ion and electron cyclotron frequencies. The dispersion relation for the LH wave is  $\omega_0^2 = \omega_{\text{LH}}^2 \times (1 + (m_i/m)k_{0\parallel}^2/k_0^2)$ . This wave imparts oscillatory velocity to electrons

$$\mathbf{v}_{0\perp} = -\frac{m}{eB^2} \left( i\omega_0 \nabla_{\perp} \phi_0 - \frac{e}{m} \mathbf{B} \times \nabla_{\perp} \phi_0 \right), \quad (2)$$

$$\mathbf{v}_{0\parallel} = -\frac{e}{mi\omega_0} \nabla_{\parallel} \phi_0.$$

The second term in  $\mathbf{v}_{0\perp}$  represents the  $\mathbf{E} \times \mathbf{B}$  drift, which is much larger than the polarization drift (first term in the same equation). This oscillatory velocity provides a coupling between the low frequency TEM of potential

$$\phi = A e^{-i(\omega t - \mathbf{k} \cdot \psi)}, \quad (3)$$

and LH wave sidebands of potential

$$\phi_j = A_j e^{-i(\omega_j t - \mathbf{k}_j \cdot \psi)}, \quad (4)$$

with  $j=1$  and  $2$ , where  $\omega_1 = \omega - \omega_0$ ,  $\omega_2 = \omega + \omega_0$ ,  $\mathbf{k}_1 = \mathbf{k} - \mathbf{k}_0$ , and  $\mathbf{k}_2 = \mathbf{k} + \mathbf{k}_0$ . The linear response of electrons to the sidebands turns out to be

$$\mathbf{v}_{j\perp} = -\frac{m}{eB^2} \left( i\omega_j \nabla_{\perp} \phi_j - \frac{e}{m} \mathbf{B} \times \nabla_{\perp} \phi_j \right), \quad (5)$$

$$\mathbf{v}_{j\parallel} = -\frac{e}{mi\omega_j} \nabla_{\parallel} \phi_j.$$

## III. NONLINEAR LOW FREQUENCY RESPONSE

The pump and sidebands exert a low frequency ponderomotive force  $\mathbf{F}_p$  on electrons.  $\mathbf{F}_p$  has two components, perpendicular and parallel to the magnetic field. The response of electrons to  $\mathbf{F}_{p\perp}$  is strongly suppressed by the magnetic field and is usually weak. In the parallel direction, the electrons can effectively respond to  $F_{p\parallel}$ , hence, low frequency nonlinearity at  $\omega, \mathbf{k}$  arises mainly through  $F_{p\parallel} = -m\mathbf{v} \cdot \nabla v_{\parallel}$ . The parallel ponderomotive force, using the complex number identity  $\text{Re } \mathbf{A} \times \text{Re } \mathbf{B} = (1/2)\text{Re}[\mathbf{A} \times \mathbf{B} + \mathbf{A}^* \times \mathbf{B}]$ , for the background electrons can be written as

$$F_{p\parallel} = eik_{\parallel} \phi_p = -\left(\frac{m}{2}\right) (\mathbf{v}_{0\perp} \cdot \nabla_{\perp} v_{1\parallel} + \mathbf{v}_{1\perp} \cdot \nabla_{\perp} v_{0\parallel}) - \left(\frac{m}{2}\right) \times (\mathbf{v}_{0\perp}^* \cdot \nabla_{\perp} v_{2\parallel} + \mathbf{v}_{2\perp} \cdot \nabla_{\perp} v_{0\parallel}^*). \quad (6)$$

Using Eqs. (2) and (5) and considering only the dominant  $\mathbf{E} \times \mathbf{B}$  drift terms, the ponderomotive potential  $\phi_p$  in the limit  $\omega \ll k_{\parallel} v_{\text{the}}$  takes the form

$$\phi_{p\parallel} = -\frac{\phi_0 \phi_1}{2B^2} \frac{\mathbf{B} \times \mathbf{k}_{0\perp} \cdot \mathbf{k}_{1\perp}}{\omega_0 \omega_1 i k_{\parallel}} [\omega_0 k_{1\parallel} - \omega_1 k_{0\parallel}] - \frac{\phi_0^* \phi_2}{2B^2} \frac{\mathbf{B} \times \mathbf{k}_{0\perp} \cdot \mathbf{k}_{2\perp}}{\omega_0 \omega_2 i k_{\parallel}} [\omega_0 k_{2\parallel} - \omega_2 k_{0\parallel}]. \quad (7)$$

One may note that  $\phi_p$  is maximum when  $\mathbf{k}_{\perp}$  and  $\mathbf{k}_{0\perp}$  are perpendicular to each other. The ponderomotive force on ions is weak, hence we ignore it and take the ion response to be linear. The electron density perturbation due to  $\phi$  and  $\phi_p$  can be written in terms of electron susceptibility of  $\chi_e$  as

$$\frac{\delta n_e}{n} = \frac{k^2 \epsilon_0}{e} \chi_e (\phi + \phi_p), \quad (8)$$

whereas ion perturbation in terms of ion susceptibility  $\chi_i$  can be written as

$$\frac{\delta n_i}{n} = -\frac{k^2 \epsilon_0}{e} \chi_i \phi. \quad (9)$$

Here  $n$  is the equilibrium electron density and  $\epsilon_0$  is the free space permittivity. For the ions, neglecting collisions, longitudinal motion, and cross field guiding center drifts, one can write

$$\chi_i = \frac{2\omega_{pi}^2}{k^2 v_{thi}^2} \left[ 1 - \left( 1 - \frac{\omega_i^*}{\omega} \right) I_0 e^{-b} - \eta_i \frac{\omega_i^*}{\omega} b (I_0 - I_1) e^{-b} \right], \quad (10)$$

where  $b = (k_{\perp} \rho_i)^2$ ,  $\rho_i = v_{thi} / \omega_c$ ,  $I_0$  and  $I_1$  are the modified Bessel functions of zero and first order, respectively,  $\omega_i^*$  is the ion diamagnetic drift frequency, and  $\mathbf{k}_{\perp}$  is the perpendicular wave number where  $\mathbf{k}_{\perp} = k_{\theta} \mathbf{e}_{\theta} + k_r \mathbf{e}_r$ . For the electron susceptibility we consider two cases.

### A. CTEM

In this case susceptibility can be taken from Ref. 16,

$$\chi_e = \frac{2\omega_p^2}{k^2 v_{\text{the}}^2} \left[ 1 + \left( \frac{\epsilon}{2} \right)^{1/2} \left( 1 - \frac{\omega_e^*}{\omega} \right) \Delta \ln \frac{x_t}{\Delta} \left( g_n \sqrt{\frac{i\mu}{\pi}} \right) \right], \quad (11)$$

where  $\Delta$  is the separation of adjacent mode rational surfaces for fixed toroidal mode number,  $\Delta = 1/k_{\theta}\hat{s}$  (it also signifies the trapped electron layer width, which demarks the region in which the trapped electron response is significant),  $x_t = \sqrt{L_n/L_s}\rho$  represents the turning point width,  $L_s$ ,  $L_n$ , and  $\rho$  are the magnetic shear length, equilibrium density scale length, and ion Larmor radius and for the collisionless regime ( $\omega_{De} < \omega < \omega_b$ ),

$$\text{Im}(g_n) = 2\sqrt{\pi} \left( \frac{\omega}{\omega_{De}} \right)^{3/2} e^{-\omega/\omega_{De}}, \quad (12)$$

with  $\omega_{De} = L_n/R\omega_e^*$  and  $\omega_e^*$  is the electron diamagnetic frequency.

Using the Eqs. (10) and (11) in Poisson's equation, we obtain

$$\epsilon\phi = -\chi_e\phi_p, \quad (13)$$

where  $\epsilon = 1 + \chi_i + \chi_e$ .

### B. Weakly collisional TEM

In the low collisionality *banana* regime  $\nu_{*e} = \nu_e/\omega_{be}\epsilon \ll 1$ , where  $\nu_e$  is the 90° Coulomb collision frequency and  $\omega_{be} = \epsilon^{1/2}v_{\text{the}}/Rq$  is the typical bounce frequency of trapped electrons and electron susceptibility, and can be written as<sup>32</sup>

$$\chi_e^c = \frac{2\omega_p^2}{k^2 v_{\text{the}}^2} \left\{ 1 - \frac{2\sqrt{2}\epsilon}{\pi} \left( 1 - \frac{\omega_e^*}{\omega^c} \right) + \frac{2\sqrt{2}\epsilon\Gamma(3/4)}{\pi^{3/2}} \times (1+i) \sqrt{\frac{\nu_{\text{the}}}{\omega^c\epsilon}} \left[ 1 - \frac{\omega_e^*}{\omega^c} \left( 1 - \frac{3}{4}\eta_e \right) \right] \right\}, \quad (14)$$

where  $\nu_{\text{the}}$  is the collision frequency at thermal speed and we have neglected a small population of low energy electrons which are highly collisional. Using Eqs. (10) and (14) in Poisson's equation we obtain

$$\epsilon^c\phi = -\chi_e^c\phi_p, \quad (15)$$

where  $\epsilon^c = 1 + \chi_i + \chi_e^c$  and  $\chi_e^c$  is the electron (weakly collisional).

### IV. NONLINEAR RESPONSE AT THE SIDEBANDS

The density perturbation at  $(\omega, \mathbf{k})$  couples with the oscillatory velocity of electrons,  $\mathbf{v}_0$ , to produce nonlinear density perturbations at sideband frequencies. Solving the equation of continuity,

$$\frac{\partial}{\partial t} n_1^{\text{NL}} + \nabla \cdot \left( \frac{\delta n_e}{2} \mathbf{v}_0^* \right) = 0, \quad (16)$$

one obtains

$$n_1^{\text{NL}} = \frac{\delta n_e}{2\omega_1} (\mathbf{k}_1 \cdot \mathbf{v}_0^*). \quad (17)$$

Similarly for the upper sideband the nonlinear density perturbation can be written as

$$n_2^{\text{NL}} = \frac{\delta n_e}{2\omega_2} (\mathbf{k}_2 \cdot \mathbf{v}_0). \quad (18)$$

Using Eqs. (17) and (18) in Poisson's equation for the sideband waves, we obtain

$$\epsilon_1\phi_1 = \frac{k^2}{k_1^2} (1 + \chi_i) \frac{\mathbf{k}_1 \cdot \mathbf{v}_0^*}{2\omega_1} \phi, \quad (19)$$

$$\epsilon_2\phi_2 = \frac{k^2}{k_2^2} (1 + \chi_i) \frac{\mathbf{k}_2 \cdot \mathbf{v}_0}{2\omega_2} \phi,$$

where

$$\epsilon_1 = 1 + \frac{\omega_p^2}{\Omega_c^2} - \frac{\omega_{pi}^2}{\omega_1^2} \left( 1 + \frac{k_{1\parallel}^2 m_i}{k_1^2 m} \right), \quad (20)$$

$$\epsilon_2 = 1 + \frac{\omega_p^2}{\Omega_c^2} - \frac{\omega_{pi}^2}{\omega_2^2} \left( 1 + \frac{k_{2\parallel}^2 m_i}{k_2^2 m} \right),$$

are the dielectric functions at  $(\omega_1, \mathbf{k}_1)$  and  $(\omega_2, \mathbf{k}_2)$ .

### V. GROWTH RATE

The coupled Eqs. (13) and (19) lead to the nonlinear dispersion relation,

$$\epsilon = - \frac{\chi_e(1 + \chi_i) k^2 U^2 \sin^2 \delta \left( \frac{1}{\epsilon_1} + \frac{1}{\epsilon_2} \right)}{\left( 1 + \frac{k_{0\perp}^2}{k_{\perp}^2} \right) 4\omega_0^2}, \quad (21)$$

where  $U = |k_0\phi_0/B|$  is the magnitude of  $\mathbf{E}_0 \times \mathbf{B}$  electron velocity, and  $\delta$  is the angle between  $\mathbf{k}_{\perp}$  and  $\mathbf{k}_{0\perp}$ . For  $\omega k_{0z}/\omega_0 k_z \ll 1$ ,  $k_{\perp}^2 < k_{0\perp}^2$ , and  $k_z^2 < k_{0z}^2$ , one may write

$$\frac{1}{\epsilon_1} + \frac{1}{\epsilon_2} \simeq \frac{1}{2(1 + \omega_p^2/\Omega_c^2)} \frac{1 - k_{\perp}^2 k_{0z}^2/k_z^2 k_{0\perp}^2}{(1 - \omega_{\text{LH}}^2/\omega_0^2)}. \quad (22)$$

We simplify Eq. (21) in two different cases.

### A. CTEM

Writing  $\omega = \omega_r + i\gamma$ , with  $\gamma \ll \omega_r$ , the real and imaginary parts of Eq. (21) gives

$$\omega_r = -\omega_i^* \frac{[I_0 e^{-b} - \eta_i b (I_0 - I_1) e^{-b}]}{1 - I_0 e^{-b} + \frac{1}{T_e/T_i + P2\omega_{pi}^2/k^2 v_{\text{the}}^2}},$$

for  $b < 1$ ,

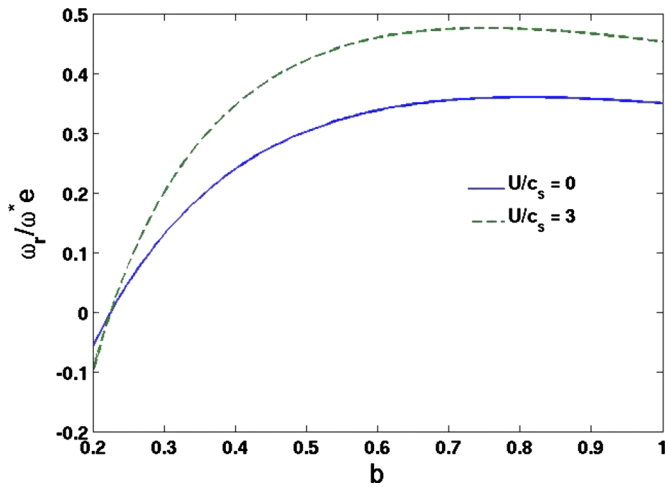


FIG. 1. (Color online) Variation of normalized real frequency for CTEM as a function of  $b$  for  $\eta_i=5$  and  $R/L_n=1.8$ .

$$\omega_r \approx -\omega_i^* \left( \frac{1-b-\eta_i b}{b + \frac{1}{T_e/T_i + P2\omega_{pi}^2/k^2v_{thi}^2}} \right), \quad (23)$$

$$\gamma = -\frac{T_i}{T_e} \sqrt{\frac{\epsilon}{2}} \frac{\left(1 - \frac{\omega_e^*}{\omega}\right) \Delta \ln \frac{x_i}{\Delta} \text{Im} \left( g_n \sqrt{\frac{i\mu}{\pi}} \right) (1 + P\chi_i)}{1 - I_0 e^{-b} + \frac{1}{(T_e/T_i) + (P2\omega_{pi}^2/k^2v_{thi}^2)}}. \quad (24)$$

There are two regimes. For small  $k_\perp$  regime,  $P$  reduces, hence the drift wave frequency enhance and growth rate increases. For large  $k_\perp$ ,  $P$  become positive and hence the growth rate reduces, where

$$P \approx \frac{1 - k_\perp^2 k_{0z}^2 / k_z^2 k_{0\perp}^2}{2(1 + \omega_p^2 / \Omega_c^2)(1 - \omega_{LH}^2 / \omega_0^2)} \frac{k^2 U^2}{4\omega_0^2(1 + k_0^2/k^2)}. \quad (25)$$

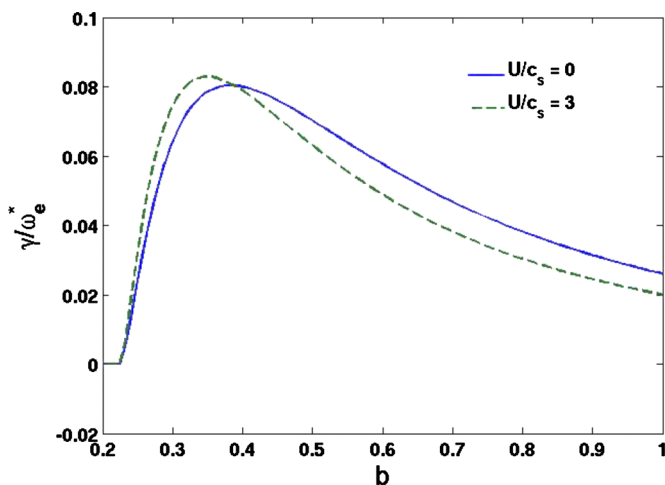


FIG. 2. (Color online) Variation of normalized growth rate for CTEM as a function of  $b$  for  $\eta_i=5$  and  $R/L_n=1.8$ .

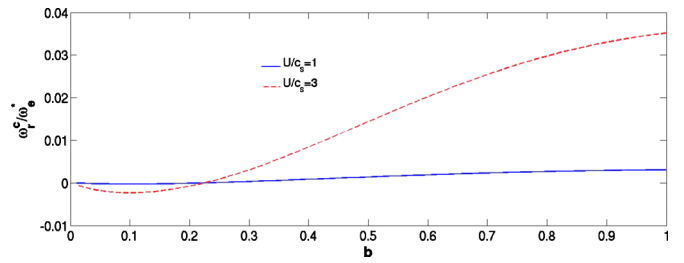


FIG. 3. (Color online) Variation of normalized real frequency for weakly collisional TEM as a function of  $b$  for two different values of LH amplitude  $U/c_s=1$  and 3. Other parameters are  $\eta_i=5$ ,  $R/L_n=1.8$ , and collisionality parameter  $L_n v_{the}/v_{thi}=0.01$ .

## B. Weakly collisional TEM

Writing  $\omega^c = \omega_r^c + i\gamma^c$ , with  $\gamma^c \ll \omega_r^c$ , the real and imaginary parts of Eq. (21) give

$$\omega_r^c \left[ \frac{G}{\omega_e^*} - \left(1 - \frac{3}{4}\eta_e\right) \left(S + \frac{1}{P}\right) \right] + \frac{G}{\Gamma(3/4)} \sqrt{\frac{\pi\epsilon}{\nu_{the}}} \sqrt{\omega_r^c} - G \left(1 - \frac{3}{4}\eta_e\right) = 0, \quad (26)$$

$$\gamma^c = \frac{\frac{G}{\Gamma(3/4)} \sqrt{\frac{\pi\epsilon}{\nu_{the}}} \sqrt{\omega_r^c}}{\left[ \frac{G}{\omega_e^*} - \left(1 - \frac{3}{4}\eta_e\right) \left(S + \frac{1}{P}\right) \right] - \frac{G}{2\Gamma(3/4)} \sqrt{\frac{\pi\epsilon}{\nu_{the}}} \omega_r^c},$$

where

$$G = 2 \frac{\omega_{pi}^2}{k^2 v_{thi}^2} \omega_i^* [I_0 e^{-b} - \eta_i b (I_0 - I_1) e^{-b}], \quad (27)$$

$$S = 1 + 2 \frac{\omega_{pi}^2}{k^2 v_{thi}^2} (1 - I_0 e^{-b}).$$

In order to have a numerical appreciation of results we consider the following set of parameters corresponding to Alcator C-Mod tokamak,<sup>24</sup> a compact tokamak: major radius  $R=0.67$  m, typical minor radius  $=0.21$  m,  $r/a \sim 0.4$ , background electron density is  $\sim 10^{20}$  m<sup>-3</sup>, electron temperature is  $\sim 2.5$  keV, ion temperature is  $\sim 1$  keV, magnetic field is  $\sim 5$  T, frequency of the LH pump is 4.6 GHz, and the

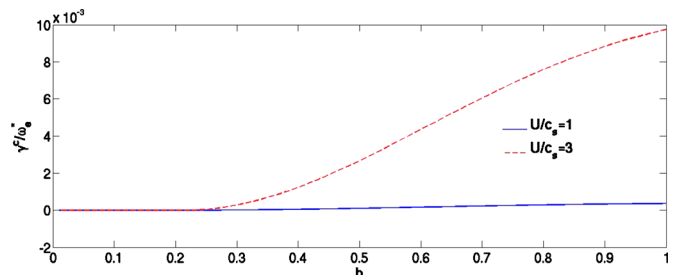


FIG. 4. (Color online) Variation of normalized growth rate for weakly collisional TEM as a function of  $b$  for two different LH amplitudes  $U/c_s=1$  and 3. Other parameters are  $\eta_i=5$ ,  $R/L_n=1.8$ , and collisionality parameter  $L_n v_{the}/v_{thi}=0.01$ .

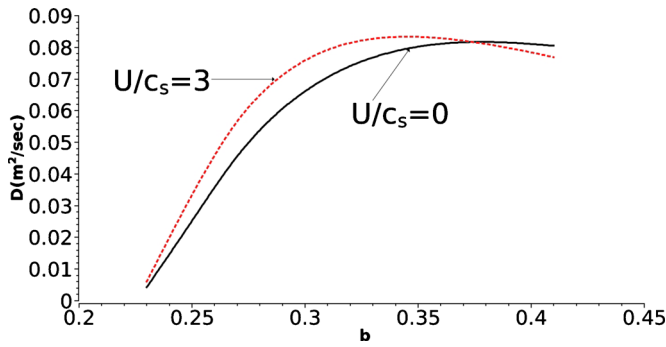


FIG. 5. (Color online) Variation of diffusion coefficient for CTEM as a function of  $b$  for  $\eta_i=5$ ,  $R/L_n=1.8$ ,  $\tau_c=20a/c_s$ , and  $U/c_s=3$ .

refractive index of the LH wave parallel to the magnetic field is  $\sim 2$ ,  $R/L_n=1.8$ , and  $U/c_s=5$ , where  $c_s$  is the ion sound speed. The value of  $U/c_s=3$  corresponds to LH power of 1.7 MW.<sup>33</sup> One may mention that the range of LH power is typically  $\sim 1$  MW and looking for the increase of LH power to 2.0–2.4 MW in future.

Figure 1 shows the progression of normalized wave frequency for electrostatic CTEM as a function of  $b$  for different pump power  $U/c_s=0$  and 3 which shows that LH pump amplitude has a significant effect on real frequency, while in the case of growth rate of the CTEM (cf. Fig. 2) the LH amplitude has a very tiny effect on the destabilization of the drift wave, and a significant effect on suppressing smaller wavelength drift wave.

Figure 3 shows the progression of normalized wave frequency for electrostatic weakly CTEM as a function of  $b$  for different LH amplitude  $U/c_s=1$  and 3, and collisionality parameter  $L_n v_{the}/v_{thi}=0.01$ . The longer wavelength drift waves are stabilized by the LH pump wave, while the shorter wavelength gets destabilized (cf. Fig. 4).

Finally we consider the anomalous diffusion in an axisymmetric system due to low frequency, electrostatic instabilities, with characteristic frequency lower than the mean bounce frequency of the trapped particles between the mirrors; the resulting resultant diffusion of the trapped particle is mainly due to the lack of conservation of the canonical angular momentum.

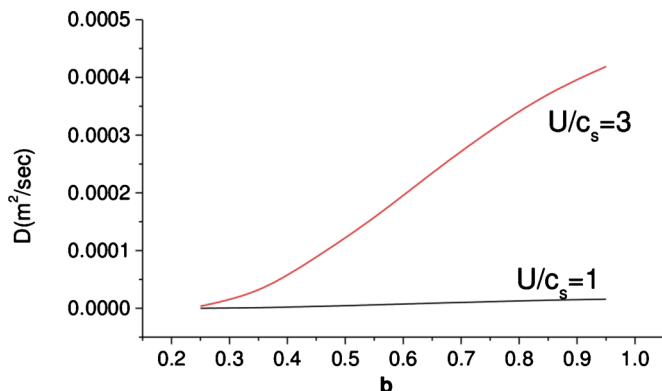


FIG. 6. (Color online) Variation of diffusion coefficient for weakly collisional TEM as a function of  $b$  for  $\eta_i=5$ ,  $R/L_n=1.8$ ,  $\tau_c=20a/c_s$ , and collisionality parameter  $L_n v_{the}/v_{thi}=0.01$ .

The anomalous diffusion coefficient for the trapped particle can be written from Refs. 26 and 34,

$$D \approx v_\Omega^2 \tau_c \approx \frac{E_\xi^2}{B_\theta^2} \tau_c, \quad (28)$$

where  $v_\Omega$  is the drift velocity of the trapped particle toward the magnetic axis and  $\tau_c$  is the correlation time. The quantitative estimate of  $|e\phi/T|^2 \sim (\gamma/\omega^*) (1/k_\perp^2 L_n^2)$ . In Figs. 5 and 6 we have plotted the diffusion coefficient for collisionless and weakly collisional TEM mode for different LH pump amplitude.

## VI. DISCUSSIONS

The anomalous diffusion of collisionless and weakly collisional trapped particles due to low frequency modes is considered. In axisymmetric torus the diffusion of the trapped particles appear due to changes in the angular momentum (Ware pinch<sup>35</sup>). With the increase of normalized LH pump amplitude it further destabilized the drift wave (cf. Figs. 3 and 4) by the parametric coupling of the pump band the sideband waves, which give a significant role in diffusion of the trapped particle in the core region of the tokamak (cf. Figs. 5 and 6), as most recently observed in Alcator C-Mod.<sup>24,25</sup> The inward diffusion of the trapped electrons in the presence of LH pump is quite significantly large compared with the weakly collisional TEMs. In the region of trapped particles the amplitude of pump wave has to be constant, which may be reasonable as long as it is equal with the pump frequency of the LH layer. The LH wave-trapped particle mode interaction is localized in a parallel length of the order of the width of the phased array of the wave guides. However the drift wave mode structure extends far beyond this region, hence the pump effectiveness may be significantly reduced. The trapped particle diffusion is primarily expected to take place in the LH resonance cone.

## ACKNOWLEDGMENTS

The authors are grateful to Professor Zhiong Lin and Dr. Yong Xiao of the University of California, Irvine for valuable suggestions.

<sup>1</sup>See [www.iter.org](http://www.iter.org).

<sup>2</sup>B. B. Kadomtsev and O. P. Pogutse, *Nucl. Fusion* **11**, 67 (1971).

<sup>3</sup>W. Horton, *Rev. Mod. Phys.* **71**, 735 (1999).

<sup>4</sup>Y. Xiao and Z. Lin, *Phys. Rev. Lett.* **103**, 085004 (2009).

<sup>5</sup>W. Deng and Z. Lin, *Phys. Plasmas* **16**, 102503 (2009).

<sup>6</sup>L. Lin, M. Porkolab, E. M. Edlund, J. C. Rost, C. L. Fiore, M. Greenwald, Y. Lin, D. R. Mikkelsen, N. Tsujii, and S. J. Wukitch, *Phys. Plasmas* **16**, 012502 (2009).

<sup>7</sup>P. H. Diamond, C. J. McDevitt, O. D. Gurcan, T. S. Hahm, W. X. Wang, E. S. Yoon, I. Holod, Z. Lin, V. Naulin, and R. Singh, *Nucl. Fusion* **49**, 045002 (2009).

<sup>8</sup>J. A. Wesson, *Tokamaks*, 3rd ed. (Clarendon, Oxford, 2004), Chaps. 2 and 8.

<sup>9</sup>E. J. Doyle, W. A. Houlberg, Y. Kamada, V. Mukhovatov, T. H. Osborne, A. Polevoi, G. Bateman, J. W. Connor, J. G. Cordey, T. Fujita, X. Garbet, T. S. Hahm, L. D. Horton, A. E. Hubbard, F. Imbeaux, F. Jenko, J. E. Kinsey, Y. Kishimoto, J. Li, T. C. Luce, Y. Martin, M. Ossipenko, V. Parail, A. Peeters, T. L. Rhodes, J. E. Rice, C. M. Roach, V. Rozhansky, F. Ryter, G. Saibene, R. Sartori, A. C. C. Sips, J. A. Snipes, M. Sughira, E.



- J. Synakowski, H. Takenaga, T. Takizuka, K. Thomsen, M. R. Wade, H. R. Wilson, ITPA Transport Physics Topical Group, ITPA Confinement Database and Modelling Topical Group, and ITPA Pedestal and Edge Topical Group, *Nucl. Fusion* **47**, S18 (2007).
- <sup>10</sup>J. W. Conner and H. R. Wilson, *Plasma Phys. Controlled Fusion* **36**, 719 (1994).
- <sup>11</sup>A. M. Dimits, G. Bateman, M. A. Beer, B. I. Cohen, W. Dorland, G. W. Hammett, C. Kim, J. E. Kinsey, M. Kotschenreuther, A. H. Kritiz, L. L. Lao, J. Mandrekas, W. M. Nevins, S. E. Parker, A. J. Redd, D. E. Shumaker, R. Sydora, and J. Weiland, *Phys. Plasmas* **7**, 969 (2000).
- <sup>12</sup>F. Jenko, W. Dorland, M. Kotschenreuther, and B. N. Rogers, *Phys. Plasmas* **7**, 1904 (2000).
- <sup>13</sup>Z. Lin, T. S. Hahm, W. W. Lee, W. M. Tang, and R. B. White, *Science* **281**, 1835 (1998).
- <sup>14</sup>J. Chowdhury, R. Ganesh, S. Brunner, J. Vaclavik, L. Villard, and P. Angelino, *Phys. Plasmas* **16**, 052507 (2009).
- <sup>15</sup>F. Y. Gang and P. H. Diamond, *Phys. Fluids B* **2**, 2976 (1990).
- <sup>16</sup>F. Y. Gang, P. H. Diamond, and M. N. Rosenbluth, *Phys. Fluids B* **3**, 68 (1991).
- <sup>17</sup>T. S. Hahm and W. M. Tang, *Phys. Fluids B* **3**, 989 (1991).
- <sup>18</sup>T. S. Hahm, *Phys. Fluids B* **3**, 1445 (1991).
- <sup>19</sup>M. A. Beer and G. W. Hammett, *Phys. Plasmas* **3**, 4018 (1996).
- <sup>20</sup>J. E. Kinsey, R. E. Waltz, and J. Candy, *Phys. Plasmas* **13**, 022305 (2006).
- <sup>21</sup>D. R. Ernst, P. T. Bonoli, P. J. Catto, W. Dorland, C. L. Firoe, R. S. Grantz, M. Greenwald, A. E. Hubbard, M. Porkolab, M. H. Redi, J. E. Rice, and K. Zhurovich, *Phys. Plasmas* **11**, 2637 (2004).
- <sup>22</sup>F. Ryter, F. Imbeaux, F. Leuterer, H. U. Fahrbach, W. Suttrop, and ASDEX Upgrade Team, *Phys. Rev. Lett.* **86**, 5498 (2001).
- <sup>23</sup>J. C. DeBoo, S. Cirant, T. C. Luce, A. Manini, C. C. Petty, F. Ryter, M. E. Austin, D. R. Baker, K. W. Gentle, C. M. Greenfield, J. E. Kinsey, and G. M. Staebler, *Nucl. Fusion* **45**, 494 (2005).
- <sup>24</sup>A. Ince-Cushman, J. E. Rice, M. Reinke, M. Greenwald, G. Wallace, R. Parker, C. Fiore, J. W. Hughes, P. Bonoli, S. Shiraiwa, A. Hubbard, S. Wolfe, I. H. Hutchinson, E. Marmor, M. Bitter, J. Wilson, and K. Hill, *Phys. Rev. Lett.* **102**, 035002 (2009).
- <sup>25</sup>J. E. Rice, A. C. Ince-Cushman, P. T. Bonoli, M. J. Greenwald, J. W. Hughes, R. R. Parker, M. L. Reinke, G. M. Wallace, C. L. Fiore, R. S. Grantz, A. E. Hubbard, J. H. Irby, E. S. Marmor, S. Shiraiwa, S. M. Wolfe, S. J. Wukitch, M. Bitter, K. Hill, and J. R. Wilson, *Nucl. Fusion* **49**, 025004 (2009).
- <sup>26</sup>C. S. Liu, D. C. Baxter, and W. B. Thompson, *Phys. Rev. Lett.* **26**, 621 (1971).
- <sup>27</sup>C. S. Liu and V. K. Tripathi, *Phys. Fluids* **23**, 345 (1980).
- <sup>28</sup>G. Praburam, V. K. Tripathi, and V. K. Jain, *Phys. Fluids* **31**, 3145 (1988).
- <sup>29</sup>K. L. Wong and P. M. Bellan, *Phys. Fluids* **21**, 841 (1978).
- <sup>30</sup>M. H. Redi, W. Dorland, C. L. Fiore, J. A. Baumgaertel, E. M. Belli, T. S. Hahm, G. W. Hammelt, and G. Rewoldt, *Phys. Plasmas* **12**, 072519 (2005).
- <sup>31</sup>A. Kuley and V. K. Tripathi, *Phys. Plasmas* **16**, 032504 (2009).
- <sup>32</sup>J. W. Connor, R. J. Hastie, and P. Helander, *Plasma Phys. Controlled Fusion* **48**, 885 (2006).
- <sup>33</sup>C. S. Liu, V. K. Tripathi, V. S. Chan, and V. Stefan, *Phys. Fluids* **27**, 1709 (1984).
- <sup>34</sup>P. Helander and D. J. Sigmar, *Collisional Transport in Magnetized Plasmas* (Cambridge University Press, Cambridge, 2002).
- <sup>35</sup>A. A. Ware, *Phys. Rev. Lett.* **25**, 15 (1970).